Activation of DNA-PK by hairpinned DNA ends reveals a stepwise mechanism of kinase activation

Katheryn Meek [ORCID]*

Department of Microbiology & Molecular Genetics, and Department of Pathobiology & Diagnostic Investigation, College of Veterinary Medicine, Michigan State University, East Lansing, MI 48824, USA

ABSTRACT

As its name implies, the DNA dependent protein kinase (DNA-PK) requires DNA double-stranded ends for enzymatic activation. Here, I demonstrate that hairpinned DNA ends are ineffective for activating the kinase toward many of its well-studied substrates (p53, XRCC4, XLF, HSP90). However, hairpinned DNA ends robustly stimulate certain DNA-PK autophosphorylations. Specifically, autophosphorylation sites within the ABCDE cluster are robustly phosphorylated when DNA-PK is activated by hairpinned DNA ends. Of note, phosphorylation of the ABCDE sites is requisite for activation of the Artemis nuclease that associates with DNA-PK to mediate hairpin opening. This finding suggests a multi-step mechanism of kinase activation. Finally, I find that all non-homologous end joining (NHEJ) defective cells (whether deficient in components of the DNA-PK complex or components of the ligase complex) are similarly deficient in joining DNA double-stranded breaks (DSBs) with hairpinned termini.

INTRODUCTION

The DNA-PK holoenzyme is comprised of three polypeptides: a regulatory subunit, the DNA end-binding, Ku heterodimer (Ku70 and Ku86) and the large catalytic subunit, DNA-PKcs [1–3]. Activation of DNA-PK is exquisitely dependent on the presence of DNA double-stranded ends, that upon Ku binding, promote the association of DNA-PKcs, facilitating kinase activation [1–3]. DNA-PKcs also interacts tightly with and phosphorylates the Artemis nuclease [4,5]. Artemis's nuclease activity is completely dependent on specific DNA-PKcs autophosphorylations at six, functionally redundant sites spanning residues 2609–2647 (ABCDE cluster) within a disordered region of the protein [6–8]. ABCDE phosphorylation likely induces a conformational change that relieves Artemis's autoinhibition that is mediated by a non-catalytic C-terminal domain of Artemis

[7,9,10]. However, to date, no biological impact has been ascribed to phosphorylation of Artemis.

DNA ends with hairpinned termini are generated as coding joint intermediates during the process of VDJ recombination [11], the site-specific recombination process of developing lymphocytes that provides for a virtually infinite repertoire of antigen binding receptors [12]. These hairpinned DNA ends are opened, processed, and ultimately joined exclusively by the non-homologous end-joining pathway (NHEJ) [13]. The NHEJ specific protein complex that includes the DNA-PK holoenzyme and Artemis is responsible for both the initial 'opening' and further trimming of hairpinned termini so that the DNA ends can subsequently be joined by NHEJ's ligase complex, XRCC4 and DNA ligase IV [4].

It would seem intuitive that hairpinned ends (that are opened by DNA-PK/Artemis) would activate DNA-PK. This issue has been addressed previously. Lu *et al*. concluded that hairpinned DNA ends activate DNA-PK to phosphorylate itself and Artemis, facilitating hairpin opening [14], whereas earlier reports from Chu and colleagues concluded that hairpinned termini completely fail to activate the kinase, using a p53 peptide as a model substrate [15]. Finally, Soubeyrand *et al*. concluded that structured single strands including hairpinned double-stranded ends activated autophosphorylation of DNA-PK (resulting in kinase inhibition), which in turn, blocked efficient phosphorylation of many heterologous substrates because of the inhibition of DNA-PK activity [16]. These results might suggest that hairpinned DNA termini only selectively activate DNA-PK; no such 'selective' activation has been suggested in previous studies of DNA-PK activation.

The TelN protelomerase (from phage N15) cuts double stranded DNA at a 56-bp cleavage site leaving covalently closed ends at both termini [17]. We have recently exploited this novel restriction endonuclease to assess joining of hairpinned DNA ends in living cells [18]. An important caveat of studying the properties of DNA with hairpinned termini is preparation of DNA moieties that uniformly have covalently closed termini. Here I utilize the TelN restriction endonuclease to assess DNA-PK kinase activation *in vitro*. I find that TelN restricted DNA efficiently activates

*To whom correspondence should be addressed. Tel: +1 517 884 5361; Email: kmeek@msu.edu

autophosphorylation of DNA-PK at T2609, a site within the 'ABCDE' autophosphorylation cluster. Previous studies have demonstrated that ABCDE phosphorylation promotes end processing (6,19), and that ABCDE phosphorylation is requisite for Artemis nuclease activity both *in vitro* and in living cells (7). Thus, activation of ABCDE autophosphorylation would be completely consistent with the study of Lieber and colleagues that concluded that hairpinned DNA activates DNA-PK autophosphorylation and Artemis nuclease activity (14). Unlike ABCDE phosphorylation, I find that TelN restricted DNA minimally induces autophosphorylation of S2056, a site within the 'PQR' autophosphorylation cluster. Phosphorylation of the PQR sites limits end processing (19). Moreover, TelN restricted DNA fails to activate DNA-PK dependent phosphorylation of a variety of other substrates including p53, XRCC4, XLF and Hsp90. Thus, these data are also completely consistent with the study from Chu and colleagues (15) who concluded that hairpinned DNA does not activate DNA-PK to facilitate phosphorylation of p53. In sum, data presented here serve to clarify an important aspect of the NHEJ mechanism: how NHEJ is initiated by the activation of DNA-PK. Moreover, the observation of partial kinase activation suggests a multi-step process of kinase activation that fits well with previous studies from both my laboratory and others suggesting an allosteric mechanism for activation of DNA-PK (20,21), a multi-step process of kinase function (8).

Finally, I find that all non-homologous end joining (NHEJ) defective cells (whether deficient in components of the DNA-PK complex or components of the ligase complex) are similarly deficient in joining DNA double-stranded breaks (DSBs) with hairpinned termini. These data are consistent with previous biochemical studies that suggest that DNA end processing during NHEJ (22–25) requires the presence of downstream components of the NHEJ complex.

MATERIALS AND METHODS

Plasmids, cell culture and cell strains

293T cells were cultured in Dulbecco's modified Eagle's medium (Life Technologies) supplemented with 10% fetal bovine serum (Atlanta Biologicals, GA, USA), 2 mM L-glutamine, 0.1 mM non-essential amino acids, 1 mM sodium pyruvate, 100 U/ml penicillin, 100 µg/ml streptomycin (Life Technologies) and 10 µg/ml ciprofloxacin. 293T cells ablated for DNA-PKcs, XLF, or both XRCC4 and XLF have been described previously (26) and were validated both by Sanger sequencing and immunoblotting. Three different commercially available anti-Artemis antibodies failed to consistently detect endogenous Artemis in 293T cells. To validate ablation of Artemis, Sanger sequencing across the gRNA target site revealed small frame shift deletions in both alleles of both Artemis clones utilized. Artemis expression plasmids were constructed by inserting a full-length Artemis cDNA into pcDNA6 (Thermo-Fisher). A nuclease deficient Artemis expression construct was generated by synthesizing (IDT) and then subcloning a BamHI–EcoRV fragment that includes H35A and D37N mutations that ablate nuclease function. Artemis ablation in

293T cells was confirmed by functional complementation of VDJ coding joining in episomal assays (Supplemental Figure S1). A fluorescent I-Sce1 NHEJ, VDJ signal and coding reporters have been described previously (26) and are derived from pECFP-N1 (Clontech). The I-Sce1 substrate was modified to replace dsRED with the Crimson version of RFP, and to replace cyan fluorescent protein with the ZsGreen version of GFP. The TelN substrate was generated by ligating double-stranded oligonucleotides including TelN sites into HindIII/SalI and BamHI/XmaI sites that flank the two I-SceI sites which flank Crimson in the I-SceI reporter substrate (Figure 1A). The recombination cassette of the TelN Crimson/ZsGreen substrate was cloned into pmSCV-puro to generate a retroviral version of the substrate. TelN and I-SceI expression vectors including nuclear localization signal, V5 Tag, and codon optimized for mammalian expression) were generated by subcloning gene fragments (synthesized by IDT) into pEF6/v5his (Thermo-Fisher). RAG1 and RAG2 expression plasmids, and the hyper-RAG2 mutant (FS) expression vectors have been described previously (27).

Reagents

The TelN restriction enzyme was purchased from New England Biolabs. The DNA-PK assay system and purified human DNA-PK were purchased from Promega. This commercial source of DNA-PK is not completely pure, and potentially contains contaminating duplex DNA, which could potentially complicate interpretation. For these reasons, control kinase reactions including no DNA were included in each experiment. Pilot mass spectrometry experiments were performed as a potential additional assay to assess PQR versus ABCDE phosphorylation; however, (unlike peptides spanning the ABCDE sites) peptides spanning the PQR sites are rarely observed by mass-spectrometry [phosphosite.org lists 222 observations of phosphorylations across the ABCDE sites using mass spectrometry methods versus only 10 across the PQR sites (28)]. This is potentially explained by the large size of proteolytic fragments spanning the PQR sites. It is unlikely that this reflects any difference in actual autophosphorylations; detection of PQR phosphorylations using phospho-specific antibodies is reported more often than for any of the ABCDE sites (28), but this may reflect the quality of available antibodies (18). These pilot mass-spectrometric experiments revealed that the Promega preparation was very minimally phosphorylated within the ABCDE cluster (<10% of sites, data not shown); no peptides spanning the PQR sites were observed, confirming that mass spectrometric analyses would not be appropriate for comparing ABCDE and PQR phosphorylations, and these experiments were not pursued further.

Episomal end joining assays

Extrachromosomal fluorescent joining assays were performed on cells plated at 20–40% confluency into 24-well plates in complete medium. Cells were transfected with 0.125 µg substrate, 0.25 pEF/I-Sce1, pEF/TelN, wild type RAG1/RAG2 or core RAG1/FS per well using polyethylenimine (PEI, 1 ug/mL, Polysciences) at 2 µl/1

μg DNA. Cells were harvested 72 h after transfection and analyzed for GFP and RFP expression by flow cytometry. The percentage of recombination was calculated as the percentage of live cells expressing GFP divided by the percentage expressing RFP. Data presented represents at least three independent experiments, which each includes triplicate transfections.

DNA-PK kinase assays

The DNA-PK enzymatic assay [SignaTECT DNA-dependent protein kinase assay system, Promega] was performed according to the manufacturer's instructions except that either gel purified ClaI or TelN restricted DNA (75 ng, ∼700 bp fragment/165 pmol) was utilized instead of sheared calf thymus DNA. A detailed protocol of the kinase reaction is provided by the manufacturer, and we have previously described use of this assay system (6,8,20,29,30). Briefly, ten units purified DNA-PK were utilized per reaction. For extract kinase reactions, freeze/thaw extracts were prepared by the method described by Finnie *et al.* (31) in the following buffer (50 mM NaF, 20 mM HEPES pH 7.8, 450 mM NaCl, 25% glycerol, 0.2 mM EDTA) with the addition of protease inhibitor cocktail (Sigma, 11836170001) and phosphatase inhibitor cockatail (Pierce, A32957); 100 ug extract was utilized/reaction. 25 ul kinase reactions were incubated for 30 min at room temperature and the reaction stopped by the addition of 10 ul 7.5 M guanidine hydrochloride. 10 ul of each reaction was spotted onto SAM2 membrane (avidin impregnated membrane; Promega); washed extensively in 2 M NaCl, and then 2 M NaCl in 1% HCPO4. Phosphorylation of the biotinylated P53 peptide on the avidin membrane is assessed by scintillation counting (γ-^{32}P-ATP [3000 Ci/mmol, with unlabeled ATP, final concentration 0.1 mM] is included in the reaction as per the manufacture's protocol). Dried membranes were subjected to scintillation counting. As in many previous studies (6,8,20,29–31), DNA-PK activity is expressed as fold increase over kinase reactions with no DNA. (This is necessary because of background level of radioactivity associated with SAM2 membranes, particularly in assays using whole cell extracts.) All assays were performed in triplicate. Experiments presented are representative of no less than three independent experiments. To detect autophosphorylated DNA-PKcs or other phosphorylations, kinase reactions were stopped by the addition of SDS-PAGE loading buffer; kinase reactions were electrophoresed, gels dried and subjected to phosphorimaging. To detect phosphorylation of p53, 2 ug purified recombinant p53 (∼38 pmol) (generous gift Bill Henry, Michigan State University) was added to kinase reactions. To detect phosphorylation of XRCC4 (2 ug, ∼26 pmol dimer), XLF (2 ug,∼30 pmol dimer) or Artemis (2 ug,∼26 pmol), purified recombinant proteins described previously (6,32) were added to kinase reactions. MBP-tagged RAG heterotetramers were purified from 293T cells similar to methods described previously (33); 5 ug (∼21 pmol hetero-tetramer) wild type or 6XS>A RAG1 mutant were added to kinase reactions. Kinase reactions were analyzed by SDS-PAGE as described above.

Immunoblot analyses

Immunoblotting was performed with *in vitro* kinase reactions as described above, except that no γ−^{32}P-ATP was included. Immunoblotting was performed as described (32). Antibodies used in this study are rabbit polyclonal anti-XRCC4 (working concentration, 1:1000; Abcam, 213729), mouse anti-ATM (working concentration, 1:1000; Abcam, 2C1), rabbit anti-XLF antibody (working concentration, 1:1000; Abcam, 33499), rabbit anti-Artemis antibody (working concentration, 1:500; Thermo-Fisher, 2544588), anti-Artemis (this antibody did not detect Artemis, Cell signaling, 13381), anti-artemis (this antibody did not detect either Artemis or phosphorylated Artemis, Thermo-fisher, PA5-27112, rabbit anti-phosphoHSP90 (working concentration, 1:1000; Cell signaling, 3488), rabbit anti-phospho-S/T-Q (working concentration, 1:1000; Cell signaling, 2851 and 9607). The DNA-PKcs antibody (working concentration, 1:1000; 42-27) was the generous gift of Tim Carter. DNA-PKcs phospho-specific antibodies utilized in this study include anti-phospho-S2056 (working concentration, 1:1000; Abcam 18192, Abcam 124918), and a rabbit anti-phospho-T2609 reagent, a generous gift of Dale Ramsden (working concentration, 1:500).

LMPCR analyses of opened hairpins

293T wild type and mutant cells were transfected either with the TelN/crim/GFP substrate alone or with the TelN expression plasmid. Forty-eight hours after transfection, cells were harvested, resuspended in 400 ul of Hirt buffer 1 (10 mM Tris [pH 8.0], 1 mM EDTA, 0.6% SDS), and incubated for 15 min at room temperature before addition of 100 ul Hirt buffer 2 (10 mM Tris [pH 8.0], 1 mM EDTA, 5 M NaCl). Samples were incubated overnight at 4°C, and then spun for 10 min at 10 000*g* at 4°C. Supernatants were extracted with phenol–chloroform, ethanol precipitated, and resuspended in 50 ul of double- distilled water; 25 ul of each Hirt supernatant was ligated to 500 pmol of annealed oligonucleotides LMPCR top/LMPCR bottom at 16°C overnight. Ligated Hirt supernatants were ethanol precipitated and used in PCR amplifications with LMPCR-pcr oligo and LMPCR-linker pcr oligonucleotides for 40 cycles.

LMPCR top: 5′ GCTATGTACTACCCGGGAATTCGT **GGCGC**

LMPCR bottom: 3′ CCCTTAAGCAC

LMPCR-linker pcr oligo: 5′ GCTATGTACTACCCGG GA AT

LMPCR-pcr substrate oligo: 5′ TTGAAGGGGTAGCC GATGC

RESULTS

Purified DNA-PK is inefficiently activated by TelN cleaved DNA

We have previously utilized a panel of DNA end-joining substrates that assess episomal DNA end joining of DNA double-strand breaks (DSBs) induced by either the RAG endonuclease or the I-SceI homing endonuclease (26). In
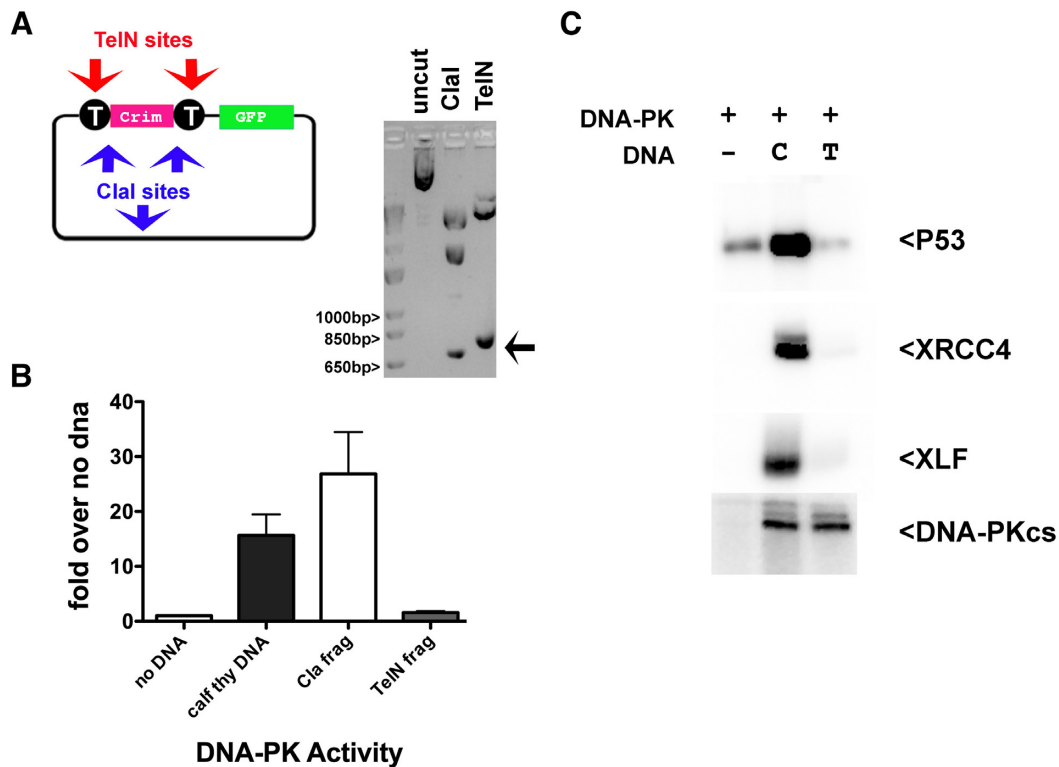
Figure 1. Purified DNA-PK is inefficiently activated by TelN cleaved DNA. (**A**) Left, schematic of TelN episomal substrate depicting position of ClaI and TelN restriction sites. Right, ethidium bromide stained 1.5% agarose gel of TelN substrate plasmid, either uncut or restricted with ClaI or TelN. (**B**) DNA-PK activity assay to quantify DNA dependent phosphorylation (using purified enzyme, Promega) of a biotinylated p53 peptide. Relative phosphorylation is shown as fold increase over reactions including no DNA. (**C**) Phosphorimager analysis of DNA-PK phosphorylation (using purified enzyme, Promega) of recombinant p53, XRCC4, XLF or itself when activated with no DNA, ClaI or TelN restricted DNA.

these plasmids, RAG or I-SceI target sites flank the coding sequence of the red fluorescent protein; DSBs at the two sites results in robust deletion of RFP and subsequent expression of another fluorescent protein positioned downstream of the recombination cassette. A plasmid substrate was prepared including TelN sites flanking RFP (in this case, the Crimson version of RFP). Similarly, sized DNA fragments were prepared and purified by restricting the TelN substrate plasmid with either ClaI (that generates ends with 5′ overhangs) or TelN that generates hairpinned ends (Figure 1A). The capacity for each DNA fragment to activate purified DNA-PK (Promega) was assessed using a common assay that measures phosphorylation of a biotinylated p53 peptide system (6,8,20,29,30). Assays were performed including no DNA, 250 ng sheared calf thymus DNA, 75 ng purified ClaI fragment or 75 ng purified TelN fragment. As can be seen, both sheared calf thymus DNA and the ClaI fragment induce robust phosphorylation of the p53 peptide. In contrast, the TelN fragment induces minimal phosphorylation of the p53 peptide that is not statistically different than including no DNA (Figure 1B).

Phosphorylation of full-length p53, XRCC4 and XLF, all well-known targets of DNA-PK, was also assessed. As can be seen, whereas the ClaI fragment induces robust phosphorylation of full-length p53, XRCC4 and XLF, the TelN fragment does not efficiently induce phosphorylation of any of these, no more than background phosphorylation observed in assays with no DNA (Figure 1C). Assays were

also performed with no p53 and autophosphorylation of DNA-PKcs was assessed by phosphor-imager analyses of SDS-PAGE gels. As can be seen, similar DNA-PKcs autophosphorylation was observed in assays with ClaI restricted DNA, and TelN restricted DNA; autophosphorylated DNA-PKcs was not observed in assays lacking DNA (Figure 1C, bottom panel). These data suggest that hairpinned DNA does not promote DNA-PK dependent phosphorylation of p53, XRCC4 or XLF but does promote DNA-PK autophosphorylation.

TelN cleaved DNA induces robust DNA-PKcs autophosphorylation of T2609, but not S2056

The component polypeptides of DNA-PK are amongst the most abundant in all human cells; thus, assessing DNA-PK dependent phosphorylation is straightforward using whole cell extracts from cultured human cells. We next assessed the capacity of the TelN and ClaI fragments to induce phosphorylation of the p53 peptide using extracts from wild type 293T cells or previously described 293T cells that lack DNA-PKcs via CRISPR mediated deletion (26). As can be seen, whereas the ClaI fragment induces robust p53 peptide phosphorylation using extracts from wild type 293T cells, the TelN fragment induces minimal p53 phosphorylation (Figure 2A). [In kinase assays using cell extracts, the activating DNA may be subjected to nuclease activity, potentially explaining the minimal p53 phosphorylation observed us-
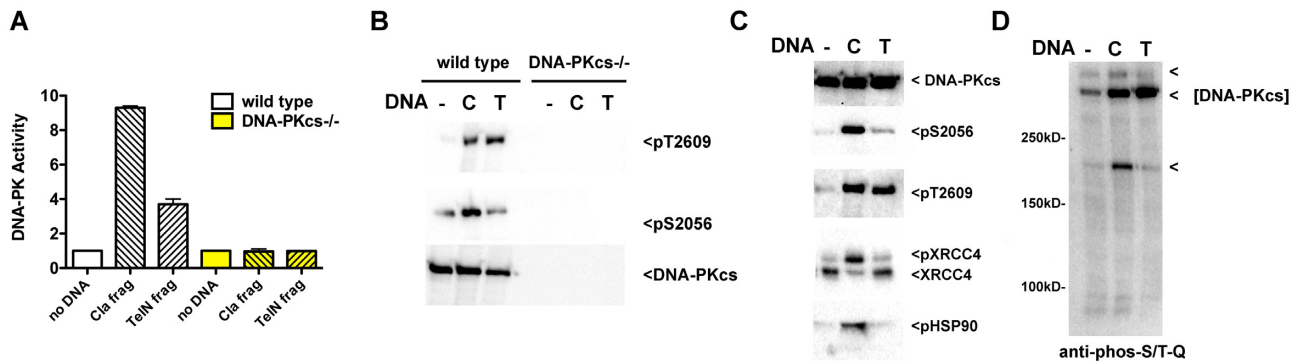
Figure 2. TelN cleaved DNA induces robust DNA-PKcs autophosphorylation of T2609, but not S2056. (**A**) DNA-PK activity assay to quantify DNA dependent phosphorylation from whole cell extracts using a biotinylated p53 peptide. Relative phosphorylation is shown as fold increase over reactions including no DNA. (**B**) Immunoblot analyses of DNA-PK kinase assays including no DNA, or ClaI or TelN restricted DNA using whole cell extracts from wild type 293T cells or DNA-PKcs ablated 293T cells. Relative phosphorylation of DNA-PKcs T2609 or S2056, versus total DNA-PKcs is presented as indicated. (**C**) Immunoblot analyses of DNA-PK kinase assays including no DNA, or ClaI or TelN restricted DNA using whole cell extracts from wild type 293T cells. Relative phosphorylation of DNA-PKcs T2609 or S2056, XRCC4 and HSP90 is presented. Total DNA-PKcs and XRCC4 is also presented as indicated. (**D**) Immunoblot analyses of DNA-PK kinase assays including no DNA, or ClaI or TelN restricted DNA using whole cell extracts from wild type 293T cells. Relative phosphorylation of proteins containing S/T-Q targets was assessed.

ing TelN restricted DNA fragment that is not observed utilizing purified enzyme.] As expected, no DNA dependent phosphorylation of the p53 peptide was observed in experiments using extracts from DNA-PKcs deficient cells (Figure 2A). DNA-PKcs autophosphorylation was assessed using phospho-specific antibodies that we have recently stringently validated (18). As can be seen, whereas both ClaI and TelN restricted DNA robustly induce autophosphorylation of T2609 (in the ABCDE cluster), while S2056 phosphorylation (in the PQR cluster) is only promoted (over the level observed with no DNA) by ClaI restricted DNA. Numerous additional *in vitro* kinase assays were analyzed via immunoblotting; whereas T2609 phosphorylation was consistently similarly induced by both TelN and ClaI restricted DNA, phosphorylation of other well-known targets of DNA-PK (XRCC4, HSP90) was only consistently and efficiently promoted (over no DNA controls) by ClaI restricted DNA. I conclude that hairpinned DNA robustly induces T2609 autophosphorylation, a phosphorylation that promotes Artemis nuclease activity. However, in cell extract assays, hairpinned DNA termini do not fully activate DNA-PK to phosphorylate XRCC4 or HSP90 or to autophosphorylate S2056.

Finally, *in vitro* kinase assays were analyzed using a polyclonal reagent that recognizes many phosphorylated S/T-Q targets (Figure 2D). As can be seen, a phospho-S/T-Q target is apparent that co-migrates with DNA-PKcs in extracts stimulated with either the ClaI fragment or the TelN fragment. Human DNA-PKcs contains 26 S/T-Q sites, 16 of which have been reported to be phosphorylated (28); five of the six ABCDE sites are S/T-Q sites whereas two of the five PQR sites are S/T-Q sites. Two additional phospho-S/T-Q targets (~600 kDa and ~200 kDa, not identified) are robustly detected that are predominately stimulated by the ClaI fragment, but not the TelN fragments.

We considered that the difference between autophosphorylation of DNA-PKcs versus phosphorylation of other protein targets could be an issue of collision frequency, and that autophosphorylation can occur via zero order kinet-

ics (since it is the same molecule). Phosphorylation of other target proteins may depend on concentration and proximity (second order kinetics). Whereas, this may explain the observed differences between autophosphorylation versus phosphorylation of XLF, XRCC4, p53 and HSP90, this cannot explain the clear difference between autophosphorylation of T2609 versus S2056. I conclude that hairpinned DNA ends induce DNA-PKcs autophosphorylation on T2609, but hairpinned termini fail to fully activate DNA-PK's enzymatic activity towards other substrates.

Hairpinned DNA termini do not stimulate DNA-PK phosphorylation of inactive Artemis

In the elegant study from Lu *et al.* (14), hairpinned DNA robustly induced phosphorylation of Artemis and DNA-PKcs. However, the authors did not address whether hairpinned DNA ends directly promote phosphorylation of Artemis, or alternatively, if the opened hairpins promote Artemis phosphorylation. Thus, I next assessed *in vitro* phosphorylation of recombinant Artemis expressed in insect cells utilized in previous studies (6). Although this recombinant Artemis interacts with DNA-PKcs in pulldown assays (6), we were unable to detect enzymatic activity with these preparations (not shown). The baculovirus derived Artemis preparations were purified via nickel affinity with buffers including imidazole; imidazole likely impairs Artemis activity (personal communication, Kefei Yu). Still, this enzymatically inactive Artemis should allow me to differentiate whether phosphorylation of Artemis is directly promoted by hairpinned ends, or alternatively, it is the opened hairpins that promote Artemis phosphorylation. Whereas ClaI restricted DNA robustly induces phosphorylation of Artemis, TelN restricted DNA does not (Figure 3A). Only a limited number of research groups have studied Artemis nuclease activity *in vitro* (4,5,7,34,35). Compelling data from Lieber *et al.* (4,5,14) unequivocally demonstrate that Artemis and DNA-PKcs form the hairpin opening activity required for VDJ recombination and likely the pri-
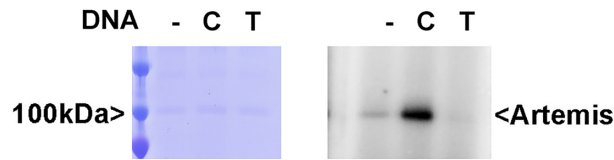
Figure 3. Hairpinned DNA termini do not stimulate DNA-PK phosphorylation of Artemis. (**A**) Phosphorimager analysis of a 6%, Coomassie blue stained SDS-PAGE gel, of DNA-PK phosphorylation (using purified enzyme, Promega) of recombinant Artemis when activated with no DNA, ClaI or TelN restricted DNA.

mary hairpin opening activity of higher eukaryotes. I suggest that whereas hairpinned termini can induce autophosphorylation of the ABCDE sites in DNA-PKcs that activate the Artemis nuclease (as shown by Lu *et al.* (14)), it is likely that the opened hairpins promote DNA-PK phosphorylation of Artemis. As with other DNA-PK targets (Figures 1 and 2), hairpinned DNA ends do not directly promote phosphorylation of enzymatically inactive Artemis (Figure 3).

DNA-PK dependent phosphorylation of RAG1 is not induced by TelN restricted DNA

Work is ongoing in my laboratory to understand the impact of DNA-PK and/or ATM phosphorylation of the RAG complex (26,36). We have discovered that RAG1 is preferentially phosphorylated by DNA-PK at the extreme non-core C-terminus. RAG-induced DSBs are the only (to my knowledge) hairpinned ends induced in normal cells; we thus considered that RAG1 phosphorylation by DNA-PK might be unique (as compared to other DNA-PK targets). Fully functional RAG tetramers were produced in 293T cells as MBP fusion proteins as depicted in Figure 4A. As can be seen, whereas robust RAG1 phosphorylation is apparent in assays including ClaI restricted DNA, little phosphorylation is induced by TelN restricted DNA (Figure 4B); only minimal RAG2 phosphorylation is observed in either condition. As expected, RAG1 with six Ser>Ala substitutions in the extreme C terminus is not phosphorylated by DNA-PK. Thus, like its other substrates, DNA-PK's phosphorylation of RAG1 is not directly promoted by hairpinned ends. Instead, I suggest that during VDJ recombination, RAG-induced hairpins induce ABCDE phosphorylation, activating the Artemis nuclease. Active Artemis cleaves the hairpinned coding termini (4); the open hairpins promote full DNA-PK activation, allowing DNA-PK to target the RAG complex.

Episomal end-joining of TelN-induced DSBs is impaired in NHEJ defective cells

Numerous studies have documented robust episomal end-joining in NHEJ deficient cells because of alternative end-joining (a-EJ) (37,38). An intensive research effort has revealed that DNA ligase III is the likely enzyme that mediates a-EJ, along with other components of the base excision repair pathway (39–41), although DNA ligase I can function in this capacity in the absence of DNA ligase III (42).

More recently, it has been shown that a-EJ is also highly reliant on DNA polymerase theta (PolQ) (43).

Unlike restriction enzyme-induced DSBs, in NHEJ deficient cells, DSBs generated during VDJ recombination by the RAG endonuclease are not efficiently joined by a-EJ. This is because the RAG complex (in an undefined manner) restricts its DSBs to NHEJ. Previously, in collaboration with Roth and colleagues, I studied a dysregulated RAG2 mutant (FS) that is partially insufficient in restraining DSBs to NHEJ (27). This RAG mutant lacks cdc2 phosphorylation sites that induce degradation of RAG2 at the G1/S border and has both increased expression levels and increased activity in cellular assays. In our previous study, we showed that with the FS RAG2 mutant, substantial joining of both coding and signal joints could be observed in rodent cells deficient in either DNA-PKcs or XRCC4. Although substantial increases were observed for both coding and signal joining, the increase in signal joining far exceeded coding joining (by ~10-fold). At the time of our previous study, it was unclear whether the difference in the level of coding and signal end joining with the RAG2 FS mutant was because the mutant still retained some ability to restrict coding ends to NHEJ as compared to signal ends; in fact further studies from Roth and colleagues documented clear deficits in the signal end complex with this RAG mutant (44). The alternative explanation was that the hairpinned coding ends were simply more difficult for a-EJ to repair, as compared to blunt signal ends. If this were the explanation, one might expect a more substantial increase in coding end joining in XRCC4 deficient cells that have an intact DNA-PKcs/Artemis complex; this was not observed. I reasoned that it might be possible to differentiate between these two possibilities by examining both RAG FS mutant hairpin joining and TelN joining in the same cell strains.

Here I utilize a panel of isogenic 293T cells with specific deficits in NHEJ (Figure 5A). [Validation of Artemis ablation was confirmed by sequence analyses and by functional complementation (Supplemental Figure S1).] Consistent with our previous study, 293T cells lacking DNA-PKcs, both XRCC4 and XLF, or harboring a kinase inactivating mutation of DNA-PKcs (Figure 5A) have severe deficiencies in both coding and signal end joining when VDJ recombination is initiated using wild type RAG1 and RAG2 ('w', Figure 1B); 293T cells deficient in Artemis have normal signal end joining but severely reduced coding end joining. When VDJ recombination is initiated with core RAG1 and the FS mutant RAG2 that is deficient in restricting DSBs to NHEJ ('m', Figure 5B), substantial coding and signal joining can be observed in all of the NHEJ defective cells (Figure 5B). Of note, although increased coding joining is observed, the increase in signal end joining is substantially higher in each of the NHEJ mutant cell strains. This difference in coding versus signal joining is consistent with our previous studies using the RAG mutant in NHEJ deficient rodent cells (27).

I next assessed hairpin versus non-hairpinned end joining using restriction enzyme-induced DSBs that are not specifically targeted to NHEJ (38) in the same panel of isogenic cell strains. The TelN cleavage site, and its mode of cleavage
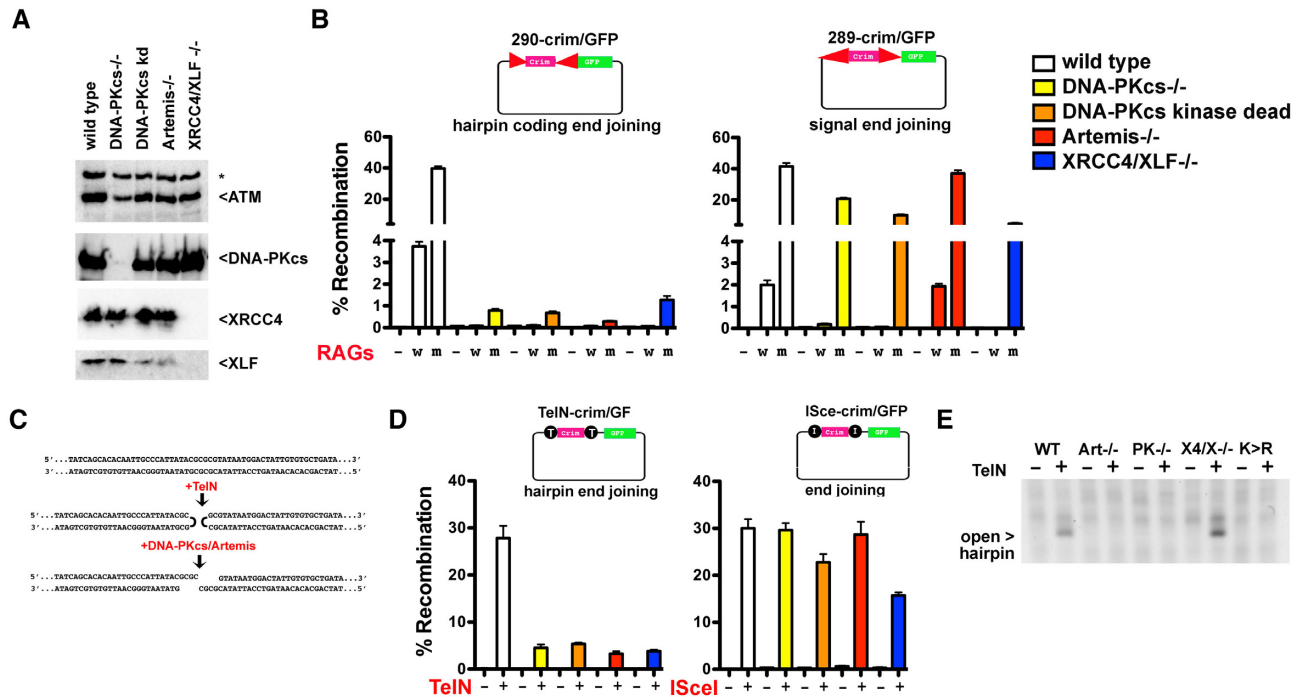
Figure 4. DNA-PK dependent phosphorylation of RAG1 is not induced by TelN restricted DNA. (**A**) Left, cartoon depicting recombinant RAG1 (ΔNR1) and RAG2 (FLR2) fusion proteins. Right, sequence comparison of RAG1's non-core extreme C-terminus; Residues depicted in red or pink, substituted to alanine residues (as reported previously (36)) in the 6X S>A RAG1 mutant. (**B**) Phosphorimager analysis of Coomassie stained 6% SDS-PAGE gel of DNA-PK phosphorylation (using purified enzyme, Promega) of recombinant wild type RAG tetramers (left) or RAG1 6X S>A when DNA-PK is activated with no DNA, ClaI or TelN restricted DNA.

is depicted in Figure 5C. From the current understanding of how the DNA-PKcs/Artemis nuclease processes hairpins (4,5), the TelN hairpins should be cleaved such that 4 base pair 3′ overhangs result; at TelN sites, this generates completely complementary ends with four base overhangs, theoretically an excellent substrate for a-EJ. As can be seen, end-joining of the I-SceI substrate (26) is robust in all cell types, and only slightly reduced in some of the NHEJ deficient cells (no >2-fold, Figure 5D). In wild type 293T cells, joining of the TelN substrate is similar to joining of the I-SceI substrate suggesting that both episomal substrates and both ectopically expressed restriction enzymes function similarly in 293T cells. In contrast, end-joining of the TelN substrate is substantially impaired (at least 5-fold) in all of the NHEJ deficient cells. The differences between I-SceI joining and TelN joining in this panel of NHEJ mutant cells is similar to the comparison of signal and coding end joining using the RAG mutant that releases its DSBs to a-EJ (Figure 5B). These data suggest that hairpinned ends cannot be joined by a-EJ. This raises the possibility that the hairpin structure of cleaved coding ends facilitates restriction of coding end joining to NHEJ during VDJ recombination.

Using a ligation mediated PCR assay (LMPCR), I assessed whether the hairpinned DNA termini of the TelN substrate are opened in each of the cell strains tested. This assay utilizes a linker that is complementary to the 4 base pair, 3′ overhang that should be generated by DNA-PKcs/Artemis-mediated opening of TelN-induced hairpins; thus the only DNA ends detected by the assay are opened TelN hairpins. As can be seen, (Figure 5E), opened hairpins are readily detected in both wild type 293T cells or cells deficient in XRCC4 and XLF; no opened hairpins

are detected in the three cell strains with deficits in either DNA-PKcs or Artemis. Of note, even though hairpinned termini are opened in XRCC4/XLF deficient cells, end-joining of the TelN substrate is similarly impaired in these cells as compared to cells that have defects in DNA-PKcs or Artemis (Figure 5D). Several previous studies utilizing biochemical approaches have suggested a link between end-processing and end ligation during NHEJ (22–25). For example, in a study assessing the capacity of the XRCC4/Lig4 complex to stimulate Artemis (even in the absence of DNA-PKcs), XRCC4/Lig4 clearly stimulated the endonuclease activity of the DNA-PKcs/Artemis complex; this stimulation was observed with each DNA end configuration tested [Gerodimos *et al.*, Figures 1–4 (22)]. Similarly, two studies demonstrated that XRCC4 is required for end processing in extract-based assays (23,24). Very recently, Loparo and colleagues demonstrated that end processing in the context of NHEJ, occurs within a 'short range synaptic complex', which requires the catalytic activity of DNA-PK, and the presence (but not enzymatic activity) of the XRCC4/LigIV complex (25). Although other explanations are possible, my results suggest that if the DNA-PKcs/Artemis complex processes hairpinned termini, those DNA ends are then restricted to joining by NHEJ, consistent with these *in vitro* studies suggesting the XRCC4/Lig4 complex is not only required for ligation but also for end-processing.

DISCUSSION

There are clearly limitations to the current study. Assessing phosphorylation using different phosphospecific antibodies (with different affinities etc) is qualitative and not quantita-

Figure 5. End-joining of TelN-induced DSBs is similarly impaired in all NHEJ defective cells. (**A**) Immunoblot analyses of whole cell extracts of 293T cells, either wild type, DNA-PKcs−/−, DNA-PKcs kinase dead, Artemis−/−, or XRCC4/XLF−/− as indicated assessing relative expression of ATM, DNA-PKcs, XRCC4 or XLF as indicated. Several commercial anti-Artemis antibodies failed to detect endogenous Artemis in 293T cells; validation of Artemis ablation was by Sanger sequencing and functional complementation (Supplemental Figure S1). (**B**) Episomal end-joining assays using either the 290-Crim/GFP (left) or 289-Crim/GFP (right) substrates. Either no RAGs, wild type RAGs, or coreRAG1/FS were co-transfected as indicated. Cells were analyzed by flow cytometry; % of cells expressing GFP/RFP is indicated as % recombination. Results were compiled from at least four experiments, with each experiment performed in triplicate for each variable. (**C**) Representation of the intact TelN cleavage site (top line), TelN cleavage site after cleavage (middle), and after DNA-PKcs/Artemis hairpin opening (bottom). (**D**) Episomal end-joining assays using either the I-SceI-Crim/GFP (left) or TelN-Crim/GFP (right) substrates. Either I-SceI or TelN was co-transfected, either alone or in combination with DNA polymerase theta as indicated. Cells were analyzed by flow cytometry; % of cells expressing GFP/RFP is indicated as % recombination. (**E**) LMPCR analyses to detect opened hairpinned ends as described in Materials and Methods.

tive. Moreover, these antibodies detect only one site in each cluster (although our previous studies demonstrate that sites within each cluster are functionally redundant (6,19)). Still, results presented here help to unify conclusions from previous studies (14–16). Whereas Smider *et al.* concluded that hairpinned DNA ends failed to activate DNA-PK, Gu *et al.* concluded that hairpinned DNA ends activated Artemis and induced phosphorylation of both Artemis and autophosphorylation of DNA-PKcs. Both studies are exactly correct. The contribution of the current study is that I show that the specific autophosphorylation of DNA-PKcs (ABCDE phosphorylation) induced by hairpinned DNA ends is exactly the phosphorylation event that is required to activate Artemis. Opened DNA ends are required to promote other DNA-PK autophosphorylations and phosphorylation of other DNA-PK targets. This unexpected finding suggests a multi-step process of kinase activation.

Previous studies have shown that Ku and DNA-PKcs efficiently assemble onto DNA ends with hairpinned termini (15). Data presented here suggest that the initial binding of free hairpinned DNA by Ku plus DNA-PKcs is sufficient to activate autophosphorylation of the ABCDE cluster, which is located in a disordered region between the N and C terminal domains (8). Lees-Miller and colleagues showed that ABCDE phosphorylation is sufficient to re-

lieve Artemis's autoinhibition facilitating hairpin opening by the Artemis endonuclease (7). In assays with hairpin activator and no Artemis, DNA-PK is not further activated, towards either the PQR sites or to exogenous substrates (Figures 1, 3A, 4). These data suggest that induction of Artemis phosphorylation by hairpinned DNA (as reported by Lu *et al.* (14)) requires hairpin opening by the Artemis nuclease. Hairpin DNA ends do not induce DNA-PK phosphorylation of inactive Artemis (Figure 3). This suggests a model whereby full kinase activation requires a free DNA end to be positioned into DNA-PK's DNA binding pocket that has been shown to be proximate to the PQR sites (21). Numerous reports have suggested that strand separation ('melting' or 'breathing' (at the DNA end-activating DNA-PK) enhances enzymatic activity (45–49). Thus, it is tempting to speculate that some degree of strand 'melting' occurs at the DNA terminus facilitating DNA-PK's ability to appropriately promote end processing. In fact, Lieber *et al.* have shown that Artemis's activity towards blunt DNA termini requires melting of the termini, likely because this provides a more suitable substrate for the nuclease (50,51). However, it seems possible that if melting promotes full kinase activation, this may promote DNA-PKcs/Artemis activity. NMR studies have shown that hairpinned termini are partially melted at the termini, but obviously the ends are still
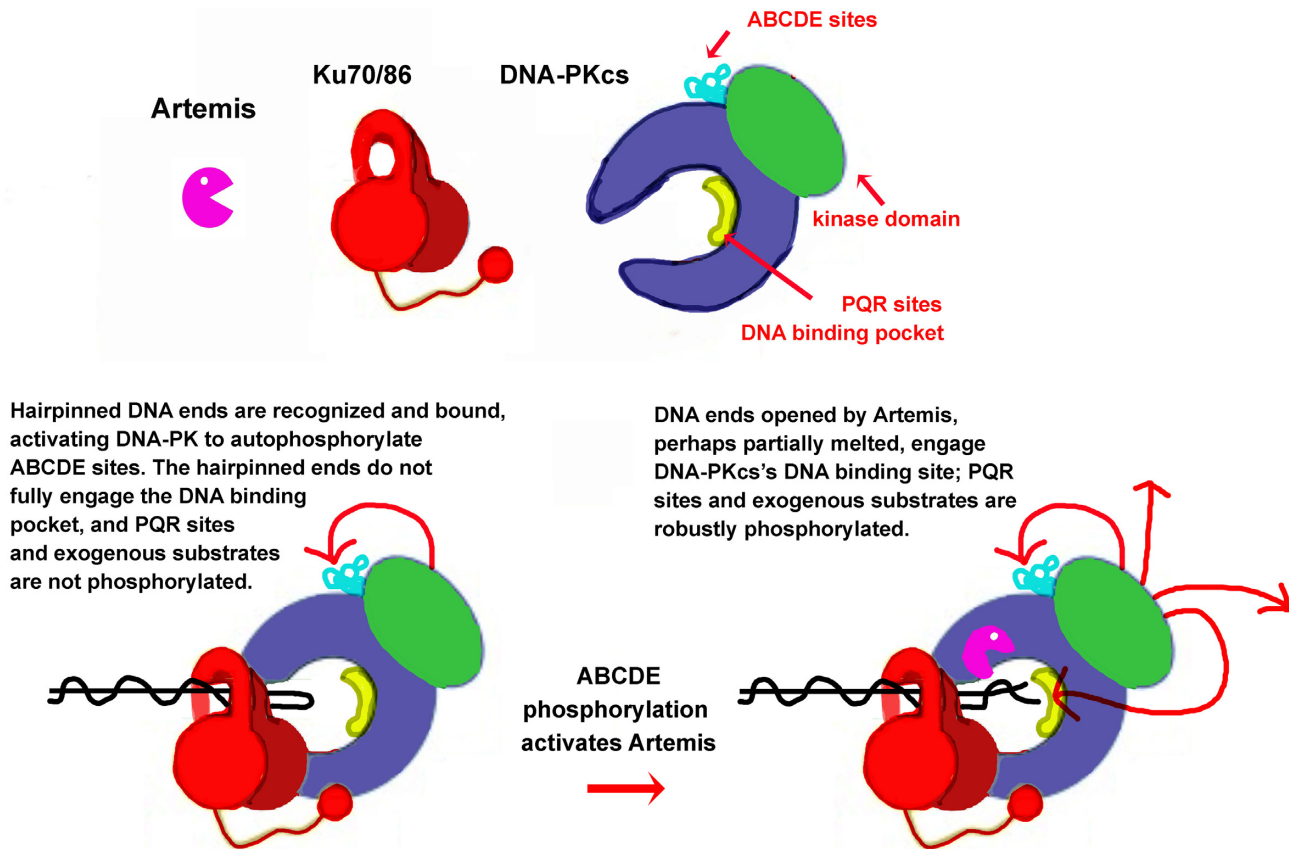
Figure 6. DNA-PK activation proceeds through mulitple steps. Hairpinned DNA ends are recognized and bound activating DNA-PK to autophosphorylate ABCDE sites. The hairpinned ends cannot fully engage the DNA binding pocket which is required to promote PQR phosphorylation and phosphorylation of exogenous substrates. ABCDE phosphorylation activates Artemis's endonuclease activity that opens the hairpin. The opened hairpin can fully engage the DNA binding pocket, fully activating DNA-PK. It seems likely that even with non-hairpinned ends, binding of the DNA end, without fully engaging the DNA binding pocket, may also result in step-wise activation of DNA-PK.

sealed. If strand separation of the DNA terminus is required for full kinase activity, this may help explain not only why hairpinned DNA does not fully activate DNA-PK, but also why DNA with cisplatin cross-links near the DNA terminus are defective in kinase activation (45).

Data presented here suggest that the a-EJ pathway cannot efficiently repair DNA hairpins that have been opened by the DNA-PKcs/Artemis complex, raising the possibility that the hairpinned structure of coding ends during VDJ recombination contributes to the complete dependence of coding end joining on NHEJ. Signal ends are also repaired primarily by NHEJ; however, in this case the stability of RAG post-cleavage complexes that sequester signal ends clearly contributes to exclusive repair by NHEJ.

There have been a number of studies using a variety of biochemical approaches demonstrating that downstream components of the NHEJ pathway are required to facilitate end processing associated with NHEJ (22–25). In cellular studies, Ramsden and colleagues proposed a model whereby the XRCC4/LigIV complex dictate end-processing depending on end configuration providing an additional link between end-processing and the XRCC4/LigIV complex (52). On the other hand, Iliakis and colleagues assessed DNA repair in cells deficient in both DNA ligase IV and Artemis and observed small additive affects, primarily in

slow repair of IR induced DSBs, but also in a-EJ assays (53) suggesting that in some cases the DNA-PKcs/Artemis complex may function independently of the XRCC4/LigIV complex. However, here, assessing resolution of hairpinned DSBs, XRCC4/XLF deficient cells although proficient in opening hairpinned termini, are similarly defective in rejoining the opened DSBs as are cells deficient in DNA-PKcs or Artemis. These data support accumulating evidence that the XRCC4/Lig4 complex is required not only for end joining but also for end processing during NHEJ.

DNA-PK is a robust kinase; hundreds of downstream targets have been identified; to date the most physiologically relevant targets identified are within DNA-PKcs itself (reviewed in (54)). Of the autophosphorylation sites in DNA-PKcs, blocking phosphorylation of the ABCDE sites has the largest functional impact. This is partially because of the absolute dependence of the Artemis nuclease on ABCDE phosphorylation (7). In addition, blocking phosphorylation of the ABCDE sites results in delayed kinetics of DNA-PK release from DSBs, resulting in slow kinetics of repair (8,19,55,56) and a much more severe cellular phenotype than simply a lack of DNA-PKcs or inactivation of its enzymatic activity. This 'slow NHEJ' phenotype has revealed that DNA-PK accesses DNA ends that arise from a variety of different DNA damaging agents including single

DNA ends that result from collapsed replication forks, suggesting additional functional roles for DNA-PKcs in repair of replication associated DNA damage (57).

We previously demonstrated that both ABCDE and PQR phosphorylations were primarily autophosphorylations and that both could occur in trans (18,30). However, in those studies, the level of trans phosphorylation was reduced compared to total phosphorylation, and we noted that it was likely that cis phosphorylation might also occur. The specific activation of ABCDE autophosphorylation by hairpinned DNA ends suggests a cis mechanism of activation, as have other studies (4,48). In sum, these previous studies along with the new findings presented here are most consistent with a cis model of ABCDE autophosphorylation.

In sum, these data suggest that DNA-PK activation proceeds through multiple distinct steps (see model, Figure 6). Assembly of Ku and DNA-PKcs onto double-stranded ends (hairpinned or not) is sufficient to promote autophosphorylation of the ABCDE sites which in turn activates Artemis, promoting end processing. However, end recognition (perhaps at 'melted' termini) is required to promote PQR autophosphorylation and full kinase activation towards DNA-PK's many substrates.

SUPPLEMENTARY DATA

Supplementary Data are available at NAR Online.

FUNDING

REFERENCES

1. Gottlieb,T.M. and Jackson,S.P. (1993) The DNA-dependent protein kinase: requirement for DNA ends and association with Ku antigen. *Cell*, **72**, 131–142.
2. Jeggo,P.A., Taccioli,G.E. and Jackson,S.P. (1995) Menage a trois: double strand break repair, V(D)J recombination and DNA-PK. *BioEssays*, **17**, 949–957.
3. Lees-Miller,S.P., Chen,Y.R. and Anderson,C.W. (1990) Human cells contain a DNA-activated protein kinase that phosphorylates simian virus 40 T antigen, mouse p53, and the human Ku autoantigen. *Mol. Cell. Biol.*, **10**, 6472–6481.
4. Ma,Y., Pannicke,U., Schwarz,K. and Lieber,M.R. (2002) Hairpin opening and overhang processing by an Artemis/DNA-dependent protein kinase complex in nonhomologous end joining and V(D)J recombination. *Cell*, **108**, 781–794.
5. Ma,Y., Schwarz,K. and Lieber,M.R. (2005) The Artemis:DNA-PKcs endonuclease cleaves DNA loops, flaps, and gaps. *DNA Repair (Amst.)*, **4**, 845–851.
6. Ding,Q., Reddy,Y.V., Wang,W., Woods,T., Douglas,P., Ramsden,D.A., Lees-Miller,S.P. and Meek,K. (2003) Autophosphorylation of the catalytic subunit of the DNA-dependent protein kinase is required for efficient end processing during DNA double-strand break repair. *Mol. Cell. Biol.*, **23**, 5836–5848.
7. Goodarzi,A.A., Yu,Y., Riballo,E., Douglas,P., Walker,S.A., Ye,R., Harer,C., Marchetti,C., Morrice,N., Jeggo,P.A. *et al.* (2006) DNA-PK autophosphorylation facilitates Artemis endonuclease activity. *EMBO J.*, **25**, 3880–3889.
8. Neal,J.A., Sugiman-Marangos,S., VanderVere-Carozza,P., Wagner,M., Turchi,J., Lees-Miller,S.P., Junop,M.S. and Meek,K. (2014) Unraveling the complexities of DNA-dependent protein kinase autophosphorylation. *Mol. Cell. Biol.*, **34**, 2162–2175.
9. Gu,J., Li,S., Zhang,X., Wang,L.C., Niewolik,D., Schwarz,K., Legerski,R.J., Zandi,E. and Lieber,M.R. (2010) DNA-PKcs regulates a single-stranded DNA endonuclease activity of Artemis. *DNA Repair (Amst.)*, **9**, 429–437.
10. Niewolik,D., Peter,I., Butscher,C. and Schwarz,K. (2017) Autoinhibition of the nuclease ARTEMIS is mediated by a physical interaction between its catalytic and C-terminal domains. *J. Biol. Chem.*, **292**, 3351–3365.
11. Roth,D.B., Menetski,J.P., Nakajima,P.B., Bosma,M.J. and Gellert,M. (1992) V(D)J recombination: broken DNA molecules with covalently sealed (hairpin) coding ends in scid mouse thymocytes. *Cell*, **70**, 983–991.
12. Gellert,M. (2002) V(D)J recombination: RAG proteins, repair factors, and regulation. *Annu. Rev. Biochem.*, **71**, 101–132.
13. Taccioli,G.E., Rathbun,G., Oltz,E., Stamato,T., Jeggo,P.A. and Alt,F.W. (1993) Impairment of V(D)J recombination in double-strand break repair mutants. *Science*, **260**, 207–210.
14. Lu,H., Shimazaki,N., Raval,P., Gu,J., Watanabe,G., Schwarz,K., Swanson,P.C. and Lieber,M.R. (2008) A biochemically defined system for coding joint formation in V(D)J recombination. *Mol. Cell*, **31**, 485–497.
15. Smider,V., Rathmell,W.K., Brown,G., Lewis,S. and Chu,G. (1998) Failure of hairpin-ended and nicked DNA To activate DNA-dependent protein kinase: implications for V(D)J recombination. *Mol. Cell. Biol.*, **18**, 6853–6858.
16. Soubeyrand,S., Torrance,H., Giffin,W., Gong,W., Schild-Poulter,C. and Hache,R.J. (2001) Activation and autoregulation of DNA-PK from structured single-stranded DNA and coding end hairpins. *PNAS*, **98**, 9605–9610.
17. Deneke,J., Ziegelin,G., Lurz,R. and Lanka,E. (2002) Phage N15 telomere resolution. Target requirements for recognition and processing by the protelomerase. *J. Biol. Chem.*, **277**, 10410–10419.
18. Neal,J.A. and Meek,K. (2019) Deciphering phenotypic variance in different models of DNA-PKcs deficiency. *DNA Repair (Amst.)*, **73**, 7–16.
19. Cui,X., Yu,Y., Gupta,S., Cho,Y.M., Lees-Miller,S.P. and Meek,K. (2005) Autophosphorylation of DNA-dependent protein kinase regulates DNA end processing and may also alter double-strand break repair pathway choice. *Mol. Cell. Biol.*, **25**, 10842–10852.
20. Meek,K., Lees-Miller,S.P. and Modesti,M. (2012) N-terminal constraint activates the catalytic subunit of the DNA-dependent protein kinase in the absence of DNA or Ku. *Nucleic Acids Res.*, **40**, 2964–2973.
21. Sibanda,B.L., Chirgadze,D.Y., Ascher,D.B. and Blundell,T.L. (2017) DNA-PKcs structure suggests an allosteric mechanism modulating DNA double-strand break repair. *Science*, **355**, 520–524.
22. Gerodimos,C.A., Chang,H.H.Y., Watanabe,G. and Lieber,M.R. (2017) Effects of DNA end configuration on XRCC4-DNA ligase IV and its stimulation of Artemis activity. *J. Biol. Chem.*, **292**, 13914–13924.
23. Lee,J.W., Yannone,S.M., Chen,D.J. and Povirk,L.F. (2003) Requirement for XRCC4 and DNA ligase IV in alignment-based gap filling for nonhomologous DNA end joining in vitro. *Cancer Res.*, **63**, 22–24.
24. Budman,J., Kim,S.A. and Chu,G. (2007) Processing of DNA for nonhomologous end-joining is controlled by kinase activity and XRCC4/ligase IV. *J. Biol. Chem.*, **282**, 11950–11959.
25. Stinson,B.M., Moreno,A.T., Walter,J.C. and Loparo,J.J. (2020) A mechanism to minimize errors during Non-homologous end joining. *Mol. Cell*, **77**, 1080–1091.
26. Neal,J.A., Xu,Y., Abe,M., Hendrickson,E. and Meek,K. (2016) Restoration of ATM expression in DNA-PKcs-Deficient cells inhibits signal end joining. *J. Immunol.*, **196**, 3032–3042.
27. Corneo,B., Wendland,R.L., Deriano,L., Cui,X., Klein,I.A., Wong,S.Y., Arnal,S., Holub,A.J., Weller,G.R., Pancake,B.A. *et al.* (2007) Rag mutations reveal robust alternative end joining. *Nature*, **449**, 483–486.
28. https://www.phosphosite.org.
29. Kienker,L.J., Shin,E.K. and Meek,K. (2000) Both V(D)J recombination and radioresistance require DNA-PK kinase activity,

though minimal levels suffice for V(D)J recombination. *Nucleic Acids Res.*, **28**, 2752–2761.

30. Meek,K., Douglas,P., Cui,X., Ding,Q. and Lees-Miller,S.P. (2007) trans Autophosphorylation at DNA-dependent protein kinase's two major autophosphorylation site clusters facilitates end processing but not end joining. *Mol. Cell. Biol.*, **27**, 3881–3890.

31. Finnie,N.J., Gottlieb,T.M., Blunt,T., Jeggo,P.A. and Jackson,S.P. (1995) DNA-dependent protein kinase activity is absent in xrs-6 cells: implications for site-specific recombination and DNA double-strand break repair. *PNAS*, **92**, 320–324.

32. Roy,S., Andres,S.N., Vergnes,A., Neal,J.A., Xu,Y., Yu,Y., Lees-Miller,S.P., Junop,M., Modesti,M. and Meek,K. (2012) XRCC4's interaction with XLF is required for coding (but not signal) end joining. *Nucleic Acids Res.*, **40**, 1684–1694.

33. Kim,M.S., Lapkouski,M., Yang,W. and Gellert,M. (2015) Crystal structure of the V(D)J recombinase RAG1-RAG2. *Nature*, **518**, 507–511.

34. Yannone,S.M., Khan,I.S., Zhou,R.Z., Zhou,T., Valerie,K. and Povirk,L.F. (2008) Coordinate 5′ and 3′ endonucleolytic trimming of terminally blocked blunt DNA double-strand break ends by Artemis nuclease and DNA-dependent protein kinase. *Nucleic Acids Res.*, **36**, 3354–3365.

35. Weterings,E., Verkaik,N.S., Keijzers,G., Florea,B.I., Wang,S.Y., Ortega,L.G., Uematsu,N., Chen,D.J. and van Gent,D.C. (2009) The Ku80 carboxy terminus stimulates joining and artemis-mediated processing of DNA ends. *Mol. Cell. Biol.*, **29**, 1134–1142.

36. Meek,K., Xu,Y., Bailie,C., Yu,K. and Neal,J.A. (2016) The ATM kinase restrains joining of both VDJ signal and coding Ends. *J. Immunol.*, **197**, 3165–3174.

37. Kabotyanski,E.B., Gomelsky,L., Han,J.O., Stamato,T.D. and Roth,D.B. (1998) Double-strand break repair in Ku86- and XRCC4-deficient cells. *Nucleic Acids Res.*, **26**, 5333–5342.

38. Cui,X. and Meek,K. (2007) Linking double-stranded DNA breaks to the recombination activating gene complex directs repair to the nonhomologous end-joining pathway. *PNAS*, **104**, 17046–17051.

39. Iliakis,G. (2009) Backup pathways of NHEJ in cells of higher eukaryotes: cell cycle dependence. *Radiother. Oncol.*, **92**, 310–315.

40. Iliakis,G., Murmann,T. and Soni,A. (2015) Alternative end-joining repair pathways are the ultimate backup for abrogated classical non-homologous end-joining and homologous recombination repair: implications for the formation of chromosome translocations. *Mutat. Res. Genet. Toxicol. Environ. Mutagen.*, **793**, 166–175.

41. Wang,H., Rosidi,B., Perrault,R., Wang,M., Zhang,L., Windhofer,F. and Iliakis,G. (2005) DNA ligase III as a candidate component of backup pathways of nonhomologous end joining. *Cancer Res.*, **65**, 4020–4030.

42. Masani,S., Han,L., Meek,K. and Yu,K. (2016) Redundant function of DNA ligase 1 and 3 in alternative end-joining during immunoglobulin class switch recombination. *PNAS*, **113**, 1261–1266.

43. Wyatt,D.W., Feng,W., Conlin,M.P., Yousefzadeh,M.J., Roberts,S.A., Mieczkowski,P., Wood,R.D., Gupta,G.P. and Ramsden,D.A. (2016) Essential roles for polymerase theta-Mediated end joining in the repair of chromosome breaks. *Mol. Cell*, **63**, 662–673.

44. Coussens,M.A., Wendland,R.L., Deriano,L., Lindsay,C.R., Arnal,S.M. and Roth,D.B. (2013) RAG2's acidic hinge restricts repair-pathway choice and promotes genomic stability. *Cell Rep.*, **4**, 870–878.

45. Pawelczak,K.S., Andrews,B.J. and Turchi,J.J. (2005) Differential activation of DNA-PK based on DNA strand orientation and sequence bias. *Nucleic Acids Res.*, **33**, 152–161.

46. Pawelczak,K.S., Bennett,S.M. and Turchi,J.J. (2011) Coordination of DNA-PK activation and nuclease processing of DNA termini in NHEJ. *Antioxid Redox Signal*, **14**, 2531–2543.

47. Pawelczak,K.S. and Turchi,J.J. (2008) A mechanism for DNA-PK activation requiring unique contributions from each strand of a DNA terminus and implications for microhomology-mediated nonhomologous DNA end joining. *Nucleic Acids Res.*, **36**, 4022–4031.

48. Jovanovic,M. and Dynan,W.S. (2006) Terminal DNA structure and ATP influence binding parameters of the DNA-dependent protein kinase at an early step prior to DNA synapsis. *Nucleic Acids Res.*, **34**, 1112–1120.

49. Hammarsten,O., DeFazio,L.G. and Chu,G. (2000) Activation of DNA-dependent protein kinase by single-stranded DNA ends. *J. Biol. Chem.*, **275**, 1541–1550.

50. Chang,H.H., Watanabe,G. and Lieber,M.R. (2015) Unifying the DNA end-processing roles of the artemis nuclease: Ku-dependent artemis resection at blunt DNA ends. *J. Biol. Chem.*, **290**, 24036–24050.

51. Chang,H.H. and Lieber,M.R. (2016) Structure-Specific nuclease activities of Artemis and the Artemis: DNA-PKcs complex. *Nucleic Acids Res.*, **44**, 4991–4997.

52. Waters,C.A., Strande,N.T., Pryor,J.M., Strom,C.N., Mieczkowski,P., Burkhalter,M.D., Oh,S., Qaqish,B.F., Moore,D.T., Hendrickson,E.A. *et al.* (2014) The fidelity of the ligation step determines how ends are resolved during nonhomologous end joining. *Nat. Commun.*, **5**, 4286.

53. Moscariello,M., Wieloch,R., Kurosawa,A., Li,F., Adachi,N., Mladenov,E. and Iliakis,G. (2015) Role for Artemis nuclease in the repair of radiation-induced DNA double strand breaks by alternative end joining. *DNA Repair (Amst.)*, **31**, 29–40.

54. Meek,K., Dang,V. and Lees-Miller,S.P. (2008) DNA-PK: the means to justify the ends? *Adv. Immunol.*, **99**, 33–58.

55. Ying,S., Chen,Z., Medhurst,A.L., Neal,J.A., Bao,Z., Mortusewicz,O., McGouran,J., Song,X., Shen,H., Hamdy,F.C. *et al.* (2016) DNA-PKcs and PARP1 bind to unresected stalled DNA replication forks where they recruit XRCC1 to mediate repair. *Cancer Res.*, **76**, 1078–1088.

56. Uematsu,N., Weterings,E., Yano,K., Morotomi-Yano,K., Jakob,B., Taucher-Scholz,G., Mari,P.O., van Gent,D.C., Chen,B.P. and Chen,D.J. (2007) Autophosphorylation of DNA-PKCS regulates its dynamics at DNA double-strand breaks. *J. Cell Biol.*, **177**, 219–229.

57. Neal,J.A., Dunger,K., Geith,K. and Meek,K. (2020) Deciphering the role of distinct DNA-PK phosphorylations at collapsed replication forks. *DNA Repair (Amst.)*, **94**, 102925.